Journal of Fluorescence, Vol. 8, No. 4, 1998

Fluorescence Properties of Donor–Acceptor-Substituted Pyrazoloquinolines

Andreas B. J. Parusel,[1] Karl Rechthaler,[1] Danuta Piorun,[2] Andrzej Danel,[3] Karen Khatchatryan,[3] Krystyna Rotkiewicz,[2,4] and Gottfried Köhler[1]

Received February 25, 1998; accepted July 13, 1998

The photophysical properties of three newly synthesized pyrazoloquinolines, composed of *N,N*-dimethylaniline as donor subunit and various substituted forms of the acceptor pyrazoloquinoline (DPPQ), were investigated by absorption as well as by stationary and time resolved fluorescence spectroscopy. These compounds show generally highly efficient emission in nonpolar and medium polar solvents; the dipole moment of the emitting state increases and the quantum yield decreases with solvent polarity. These results are explained by state reversion in polar solvents: At low polarities emission originates from a state localized on the DPPQ moiety, whereas in the high-polarity regime the next excited state of charge transfer character, in which an electron is promoted from the amino nitrogen lone pair into an excited orbital of the DPPQ moiety, becomes the fluorescent state. This view is corroborated by semiempirical calculations including the solvent reaction field, low-temperature fluorescence measurements, and the observation of effects of protonation on the spectroscopic and photophysical properties.

KEY WORDS: Photoinduced electron transfer; fluorescence anisotropy; dual fluorescence; acid–base properties.

INTRODUCTION

Dual fluorescence is often induced by polar solvents in aromatic bichromophoric systems, composed of two moieties with different redox properties and connected by a single bond [1,2]. Excitation initiates a sequence of processes which results, finally, in charge separation and involves torsional motion about the single bond connecting the two subunits. This relaxational mode slows down back electron transfer due to electronic decoupling of the two moieties. The final long wavelength fluorescing state is thus often referred to as the *twisted intramolecular charge transfer (TICT)* state [3]. This phenomenon is reminiscent of various issues such as application as highly polarity or electric field-sensitive fluorescent probes in biological systems or of organic nonlinear optical materials. As nonlinear optical effects arise from polarization of the molecules in the electric field of light, the ability of charges to be displaced within a molecule by an electric field is of crucial importance [4].

The TICT model was first proposed to explain dual fluorescence of 4-(*N,N*-dimethylamino)-benzonitrile and is well supported by the observation of the effects of stereoselective substitution influencing torsional motion about the amino-aryl single bond on the emission properties [3]. For larger donor–acceptor systems such as 9-[4-(*N,N*-dimethylamino)-phenyl]-anthracene or carba-

[1] Institut für Theoretische Chemie und Strahlenchemie der Universität Wien, Althanstrasse 14, A-1090 Vienna, Austria.
[2] Pedagogical University of Kielce, Institute of Chemistry, Chęcińska 5, PL-25-020 Kielce, Poland.
[3] H. Kołłataj Agricultural University, Al. Mickiewicza 24/28, PL-30-059 Cracow, Poland.
[4] Institute of Physical Chemistry, Polish Academy of Sciences, Kasprzaka 44, PL-01-224 Warsaw, Poland.

1053-0509/98/1200-0375$15.00/0 © 1998 Plenum Publishing Corporation

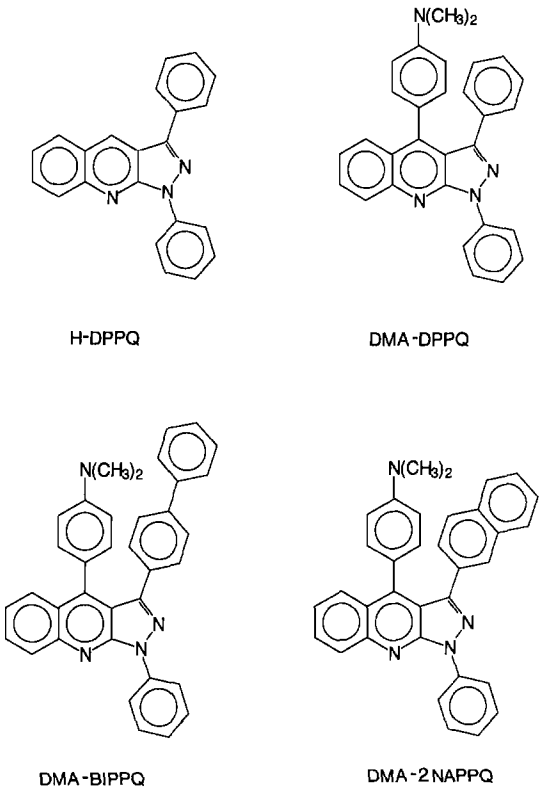

Scheme I

zole derivatives connected to various cyanophenyl moieties as acceptors, relaxation to a polar excited state with a smaller inclination angle between the two subunits compared to the ground state was postulated [5–7]. The two subunits in the symmetric biaryl 9,9'-bianthryl, perpendicular in the ground state, relax to a nonpolar excited state with a torsional angle markedly smaller than 90° in nonpolar solvents or to a charge-separated orthogonal state in polar solvents [8]. Theoretical and experimental results obtained for 4-[(4-*N*,*N*-dimethyl-amino)-phenyl]-3,5-dimethyl-1,7-diphenyl-bispyrazolo [3,4-b;4', 3'-e]-pyridine (DMA-DMPP) suggest a perpendicular charge-transfer state in accordance with the TICT state [9–11].

It has been shown that pyrazoloquinoline derivatives are efficient blue emitters with absorption in the near-ultraviolet region and with a fluorescence quantum yield near to unity. Substitution with a dimethylanilino donor group results in strongly solvent polarity-dependent fluorescence properties [12]. The singlet excited state was shown to be highly polarizable and these compounds are promising as efficient nonlinear optical materials. In the present paper we report experimental as well as theoretical investigations of the photophysical properties of various newly synthesized donor–acceptor derivatives (see Scheme I), i.e., 4-(4-*N*,*N*-dimethyl-aminophenyl)-1,3-diphenyl-pyrazolo[3,4-b]quinoline (DMA-DPPQ), 3-(4-biphenylyl)-4-(4-*N*,*N*-dimethyl-amino-phenyl)-1-phenyl-pyrazolo[3,4-b]quinoline (DMA-BIPPQ), and 4-(4-*N*,*N*-dimethylamino-phenyl)-3-(2-naphthyl)-1-phenyl-pyrazolo[3,4-b]quinoline (DMA-2NAPPQ), in comparison to the parent compound 1,3-diphenyl-pyrazolo[3,4-b]quinoline (H-DPPQ).

METHODS

Experimental

The four compounds, H-DPPQ, DMA-DPPQ, DMA-BIPPQ, and DMA-2NAPPQ (formulae in Scheme I), were synthesized by some of us (A.D., K.Ch., P.T.). The first one was obtained according to the procedure reported in Ref. 13. The synthesis of DMA-DPPQ, DMA-BIPPQ, and DMA-2NAPPQ was performed for the first time and will be described elsewhere [14].

The solvents used were of the highest available quality and checked for impurities by absorption and fluorescence spectroscopy. The following numbering of solvents is used throughout the text: hexane (1), benzene (2), toluene (3), butyl ether (4), *t*-butyl methyl ether (5), 1-chlorobutane (6), tetrahydrofuran (7), dichloromethane (8), 1,2-dichloroethane (9), pentanol-1 (10), butanol-1 (11), cyclohexanone (12), propanol-1 (13), ethanol (14), methanol (15), *N*,*N*-dimethylformamide (16), acetonitrile (17), and dimethyl sulfoxide (18). Absorption and fluorescence spectra as well as fluorescence decay times were measured as described previously [9]. Fluorescence excitation anisotropy spectra were measured with the aim of the spectrofluorimeter constructed by J. Jasny at the Institute of Physical Chemistry of the Polish Academy of Science in Warsaw [15].

Semiempirical Calculations

Ground-state geometries of all compounds are obtained by AM1 [16] calculations both with and without electron correlation using the VAMP program package, Version 6.1 [17]. Electron correlation effects are considered for the computation of ground-state as well as excited-state properties using the multielectron configuration interaction method with all single and double excitations within an active space of 10 orbitals (from the HOMO-4 to the LUMO+4). This corresponds to 876 configurations considered in the CI. The self-consistent

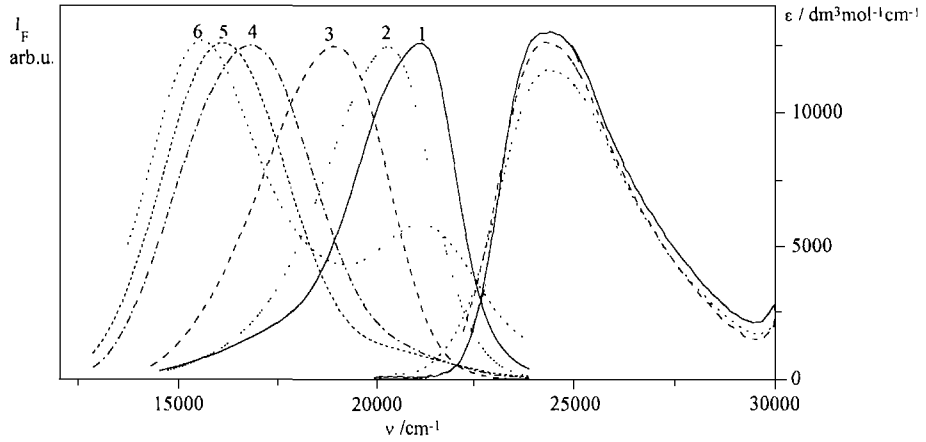

Fig. 1. Absorption and corrected normalized fluorescence spectra of DMA-DPPQ in benzene (1), 1-chlorobutane (2), dichloromethane (3), pentanol-1 (4), ethanol (5), and methanol (6).

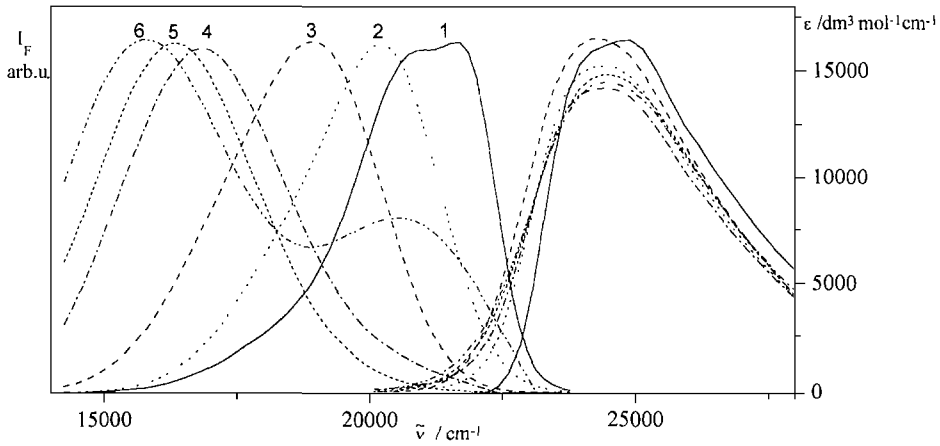

Fig. 2. Absorption and corrected normalized fluorescence spectra of DMA-BIPPQ in hexane (1), 1-chlorobutane (2), dichloromethane (3), butanol-1 (4), acetonitrile (5), and methanol (6).

reaction field (SCRF) method [18] is used for calculation of solvation effects on the spectra obtained in gas phase. For simulation of the environment electrostatic contributions are taken into account, and dispersion and free cavity energy are considered where noted in the text. All calculations are performed on SGI INDY workstations (MIPS R4400) at the University of Vienna.

RESULTS

Absorption Spectra

Absorption spectra of the four pyrazoloquinoline derivatives are presented in Figs. 1–4 and generally show weak blue-shift with increasing solvent polarity. In the case of DMA-BIPPQ (see Fig. 2) and DMA-2NAPPQ (see Fig. 3), however, a red-shift is found in low-polarity solvents like 1-chlorobutane and dichloromethane in comparison to hexane but, again, a blue-shift in solvents of higher polarity. Additionally, the absorbance on the long-wavelength edge of the first absorption band, i.e., below 22,000 cm^{-1}, increases in the order DMA-DPPQ < DMA-2NAPPQ < DMA-BIPPQ. H-DPPQ shows no such effect (see Fig. 4).

Anisotropy of Fluorescence Excitation

The fluorescence anisotropy measured at 150 K (see Fig. 5) shows a positive value ($r = +0.33$) for

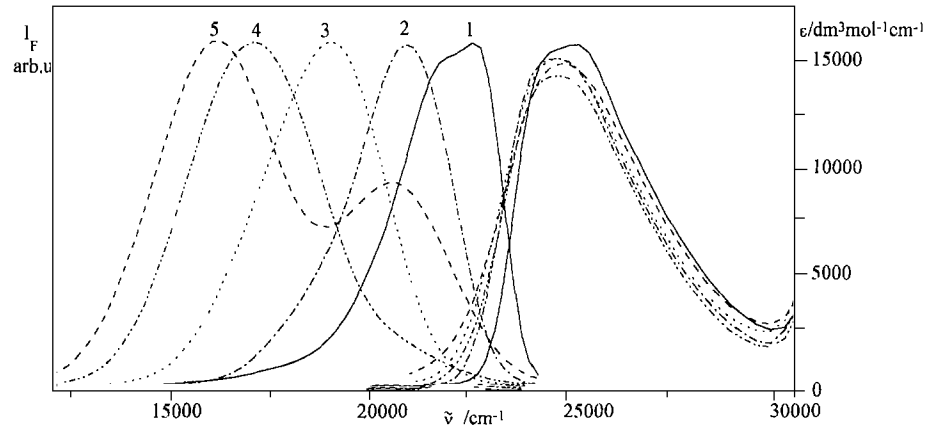

Fig. 3. Absorption and corrected normalized fluorescence spectra of DMA-2NAPPQ in hexane (1), benzene (2), dichloromethane (3), pentanol-1 (4), and methanol (5).

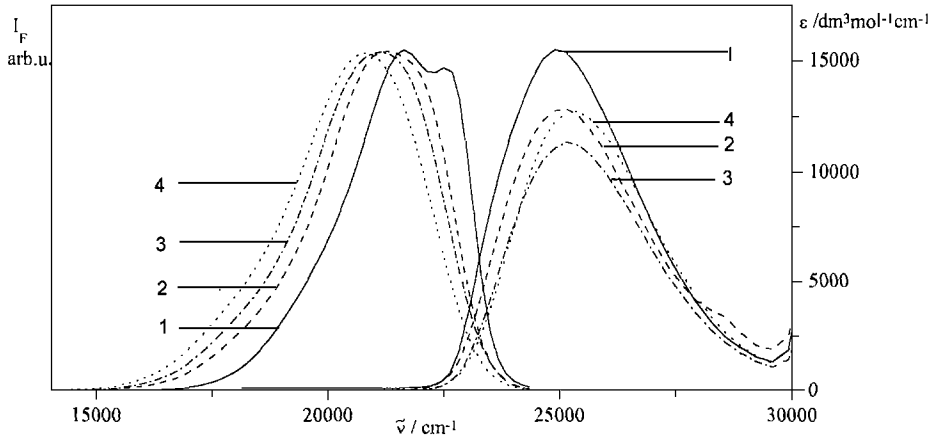

Fig. 4. Absorption and corrected normalized fluorescence spectra of H-DPPQ in hexane (1), 1-chlorobutane (2), ethanol (3), and acetonitrile (4).

excitation into the longest-wavelength band and becomes negative ($r = -0.09$) for the next band, around 31,200 cm^{-1}. It is generally constant over the whole emission range. For the third strong band the anisotropy increases again and reaches $r = +0.10$ at 35,700 cm^{-1}. Fluorescence becomes depolarized at excitation above 38,500 cm^{-1}.

Fluorescence

Room-Temperature Spectra

The fluorescence spectra of all investigated compounds are red-shifted with increasing solvent polarity. The slope of a plot of the fluorescence maximum wave numbers versus Onsager's solvent polarity function $\Delta f = (D - 1)/(2D + 1) - (n^2 - 1)/(2n^2 + 1)$ becomes considerably larger in solvents of a higher polarity than chlorobutane (see Fig. 6a). The dipole moments of the fluorescing states of the four compounds were estimated from the corresponding slopes according to the following equation [19]:

$$\tilde{\nu}_f = \tilde{\nu}_f^0 - \frac{\vec{\mu}_m (\vec{\mu}_m - \vec{\mu}_n)}{4\pi\varepsilon_0 hc\chi a^3} * \Delta f \qquad (1)$$

Equation (1) is obtained assuming a point dipole located in the center of the spherical cavity (radius a) and a solute polarizability density $\chi = 0.5$ [19]. μ_n denotes the dipole moment in ground state and μ_m that in the fluorescing state. ν_f and ν_f^0 are the fluorescence maximum

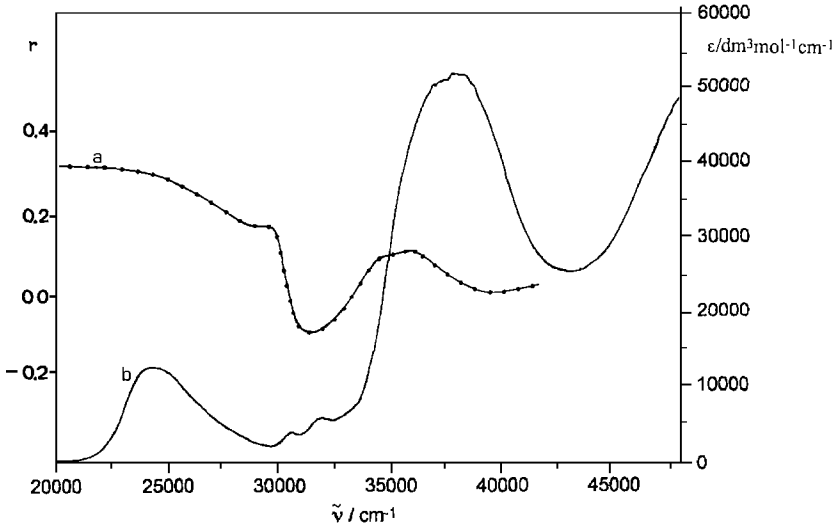

Fig. 5. Anisotropy spectrum (a) of DMA-DPPQ fluorescence excitation measured in propanol-1 at 150 K. The absorption spectrum (b) in the same solvent at room temperature is also given.

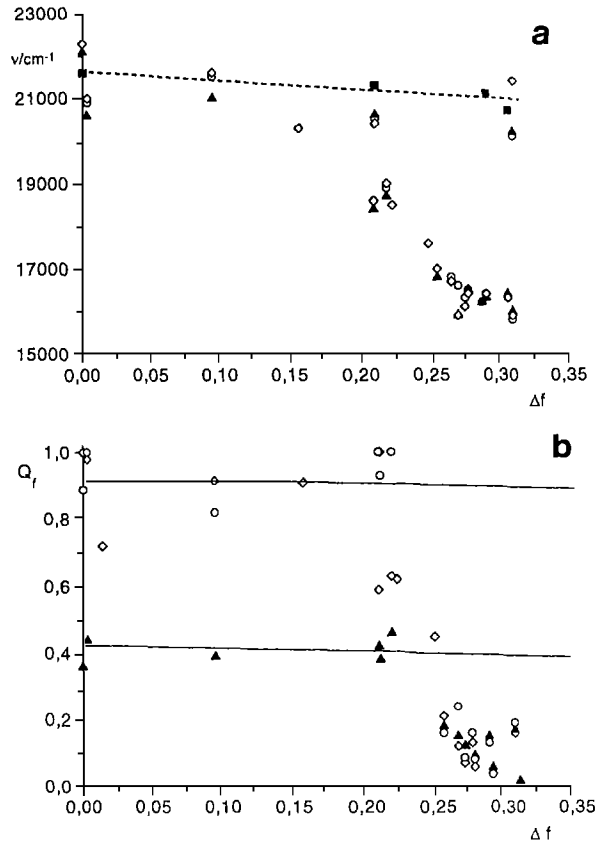

Fig. 6. Plot of (a) the wavenumber of fluorescence maxima and (b) of the fluorescence quantum yield Q_f of DMA-DPPQ (◇), DMA-BIPPQ (○), DMA-2NAPPQ (▲), and H-DPPQ (■), drawn for the same solvents as in Figs. 1–4 versus the polarity function Δf. For DMA-DPPQ some additional data in other solvents are also given.

wave numbers in solution and in vacuum, respectively. Assuming an Onsager radius a = 760 pm and a ground-state dipole moment $\mu_n = 16.0 \times 10^{-30}$ Cm, both obtained from semiempirical calculations, the dipole moment of the fluorescing state of DMA-DPPQ becomes equal to $(42 \pm 8)\ 10^{-30}$ Cm in the solvent polarity range in between $\Delta f = 0.00$ and 0.21, whereas in strongly polar solvents it becomes $93 \cdot 10^{-30}$ Cm. The values of dipole moments in the ground as well as in the excited state of DMA-BIPPQ and DMA-2NAPPQ are of similar magnitude (see Fig. 6). Fluorescence originating only from the weakly polar state is found for H-DPPQ. The fluorescence quantum yield Q_F shows a similar functional dependence on Δf as the fluorescence maximum: the slope increases strongly as Δf exceeds a value of 0.2 (see Figs. 6a and b).

In protic solvents dual fluorescence is observed for all three donor-substituted compounds, as reported for DMA-DMPP previously [9]. The high-energy band fits excellently to the solvent polarity dependence obtained for the fluorescing state with a small dipole moment, whereas the low-energy band is found at energies proposed for the highly dipolar state.

Low-Temperature Spectra

In the protic solvent propanol-1 the long-wavelength fluorescence band of DMA-DPPQ shifts to the blue and its total fluorescence quantum yield increases with decreasing temperature (see Fig. 7a). Below 230 K only a single band is resolved and its half-maximum band width (Γ_F) reaches a maximal value at 234 K (see

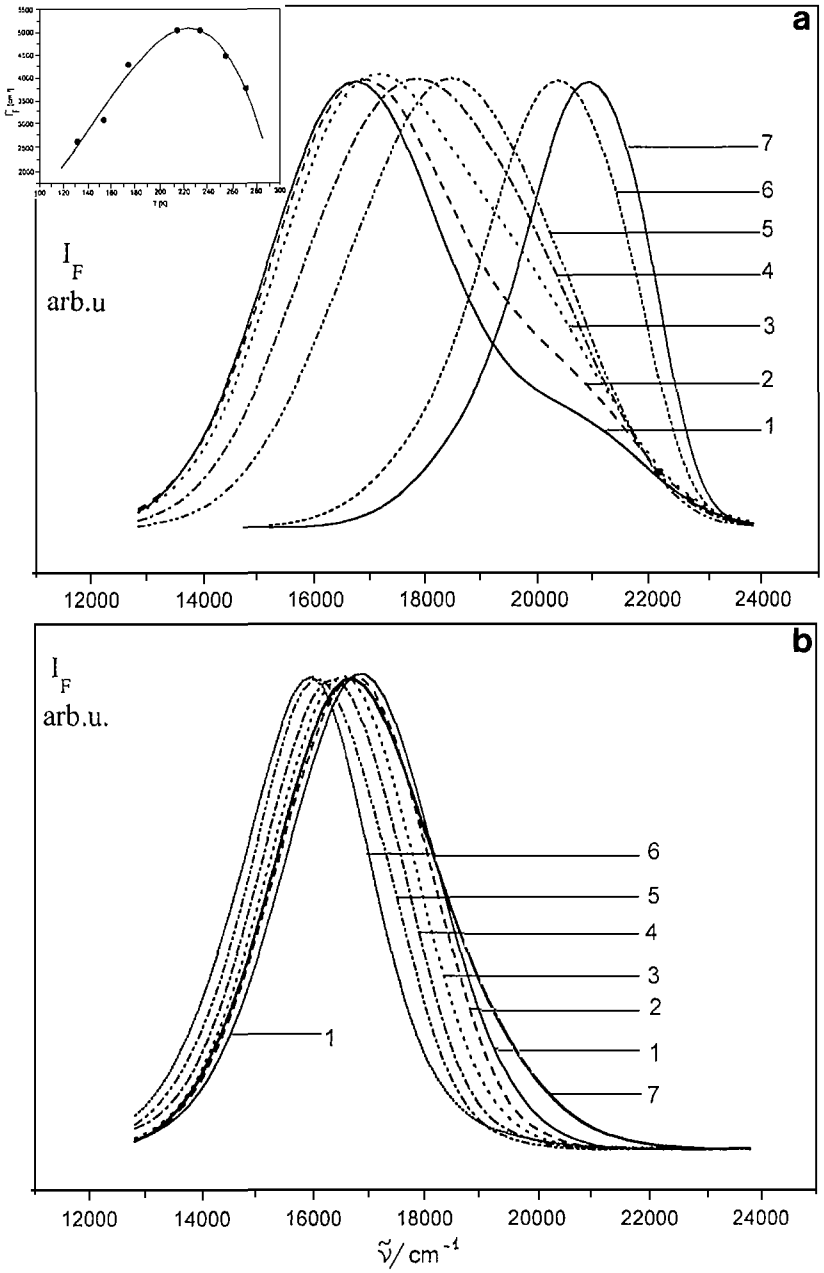

Fig. 7. Normalized corrected fluorescence spectra of DMA-DPPQ in (a) propanol-1 at (1) 272 K (1),(2) 255 K (1.67), (3) 234 K (3.0), (4) 215 K (6.5), (5) 174 K (13.3), (6) 154 K (18), and (7) 132 K (21.8) (the numbers in parentheses represent the multiplication factor to obtain the relative intensity compared/to that at 272 K taken as 1) and (b) butyronitrile at (1) 272 K (1), (2) 254 K (1), (3) 234 K (0.97), (4) 215 K (0.92), (5) 195 K (0.86), (6) 165 K (0.78), and (7) 146 K (1.35).

inset in Fig. 7a). Such behavior is most likely caused by efficient overlap of the two fluorescence band found at room temperature. In glassy solutions fluorescence is emitted exclusively from the nonrelaxed S_1 state which is characterized by a small dipole moment.

In polar aprotic butyronitrile as solvent, only a single fluorescence band is observed (see Fig. 7b), which shifts to the red with decreasing temperature, as long as the solution remains fluid and its quantum yield decreases. In glassy solution, however, the fluorescence is

remarkably blue-shifted and is found at a similar spectral position as that at room temperature. Traces of a short-wavelength emission might be indicated by the high-energy tail of the spectrum.

Absorption Spectra of Acidified Solutions

Protonation of DMA-DPPQ was investigated in solutions of acetonitrile and ethanol. The substance is only poorly soluble in water. Two steps of protonation have been observed for $5 \cdot 10^{-5}$ *M* DMA-DPPQ (see Figs. 8a and b): a first change of the spectrum appears for $HClO_4$ concentrations between 0 and $5 \cdot 10^{-5}$ *M* in acetonitrile and between 0 and $9 \cdot 10^{-2}$ *M* in ethanol (see Fig. 8c) and a second protonation step is observed above $5 \cdot 10^{-5}$ *M* $HClO_4$ in acetonitrile. In ethanol practically no additional change of the spectrum is observed at $HClO_4$ concentrations higher than 0.1 *M*.

The first protonation equilibrium in acetonitrile solutions is characterized by well-defined isosbestic points appearing at 21,000, 25,400, and 31,800 cm^{-1} as well as in connection with a new weak long-wavelength band rising at about 19,500 cm^{-1}. In ethanol solution less well-defined isosbestic points are found at 28,900 and 31,300 cm^{-1} (see Fig. 8c). No long-wavelength band is found in the latter case.

The second step, observed only in acetonitrile solutions, is characterized by a different series of isosbestic points located at 21,300, 24,000, 27,700 and 31,600 cm^{-1}. The long-wavelength band disappears at these high acid concentrations (see Fig. 8c).

Fluorescence Spectra in Acidified Solutions

The fluorescence in acetonitrile solutions and acid concentrations $<5 \cdot 10^{-5}$ *M* consists of two bands, peaking at 16,200 and 20,300 cm^{-1}. These two bands peak at 16,400 and 20,600 cm^{-1} in ethanolic solutions (see Fig. 9). No emission is observed for excitation of the 19,500 cm^{-1} long-wavelength band. If the ratio of solute/acid concentrations is 1:1 in acetonitrile solutions, only 20,300 cm^{-1} fluorescence is observed (see Fig. 9). In ethanol only for a 2000-fold excess of $HClO_4$ over the substrate concentration the long-wavelength fluorescence disappears (see Fig. 10). The second step of protonation is characterized by an efficient quenching of the short-wavelength fluorescence (see Figs. 9b and 10b) in both solvents.

Theoretical Calculations

Ground-state optimization of DMA-DPPQ results in a highly asymmetric geometry with a dipole moment of $15 \cdot 10^{-30}$ Cm oriented within the molecular plane (*xy*) and pointing from the amino to the aza nitrogen. The three phenyls (for naming of the rotational angles and numeration of the phenyls, see Scheme II) are twisted with respect to the heteroaromatic system by 74° (α), 56° (β), and 49° (γ), respectively. The two phenyls in the α and β position are almost staggered and the heteroaromatic ring system is distorted relative to a planar conformation by approximately 4° due to a sterical hindrance. The dimethylamino (DMAm) group is nearly untwisted (δ = 2°) relative to the aryl ring and a pyramidalization angle ω equal to 18° results. Small energy barriers of 2 kJ mol^{-1} were obtained for the inversion motion ω of the dimethylamino group and of 0.1 kJ mol^{-1} for the rotation α about the donor–acceptor single bond. Both α and ω show thus a shallow gradient on the energy hypersurface and are considered as 0° (ω) and 90° (α), respectively, for the succeeding calculations.

The frontier orbitals were analyzed and the highest occupied and the lowest unoccupied molecular orbitals are located mainly within the heteroaromatic subunit with differing contribution from the β and γ phenyl rings. The HOMO-1 can be described best as a π orbital located within the dimethylanilino group with significant Np_z contribution and its free electron pair character increases significantly upon rotation δ. Thus, it becomes of pure Np_z character for δ = 90°. The resulting ground- and excited-state energies and dipole moments for several different geometries are summarized in Table I. Excitation of the first excited state is characterized by the one-electron HOMO → LUMO transition, i.e., a ππ* transition within the heteroaromatic system, which yields a singlet state with a small dipole moment of $14 \cdot 10^{-30}$ Cm directed from the α phenyl to the γ phenyl moieties. Decreasing of the inversion angles ω yields a stabilization of the first excited state S_1 and the HOMO → LUMO wavefunction is mixed with increasing contributions arising from the HOMO-1 → LUMO transition rising from 3% for ω = 18° to 25% ω = 0°. Consequently, the charge transfer character of this transition increases and the dipole moment rises from 14×10^{-30} cm for ω = 18° to 41×10^{-30} cm for ω = 0°.

Localization of the HOMO-1 orbital on the dimethylamino group is achieved by large twisting angles δ. The third excited state for an angle δ = 90° is of TICT character in which one electron is transferred from the amino group to the acceptor moiety. It has a large dipole moment of 60×10^{-30} Cm but lies more than 53 kJ

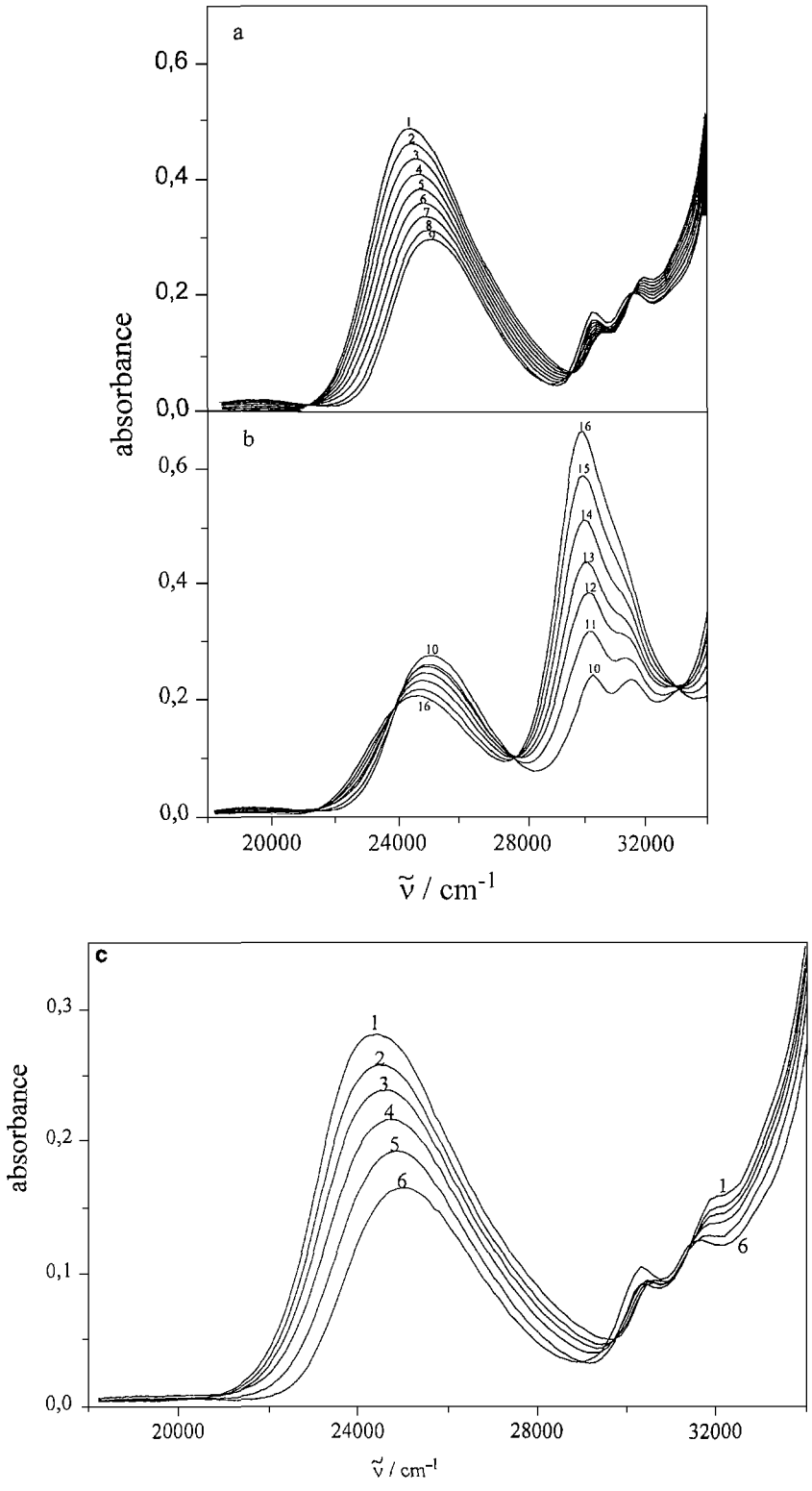

Fig. 8. Absorption spectra of acidified solutions of DMA-DPPQ ($c = 5 \times 10^{-5}$ *M*) in acetonitrile: (a) $HClO_4$ concentrations from 0 *M* (1) to $4 \cdot 10^{-5}$ *M* (9). The increment of the acid concentration is $0.5 \cdot 10^{-5}$ *M*. (b) $HClO_4$ concentrations: $5.0 \cdot 10^{-5}$ *M* (10), $6.0 \cdot 10^{-5}$ *M* (11), $7.0 \cdot 10^{-5}$ *M* (12), $8.0 \cdot 10^{-5}$ *M* (13), $1.0 \cdot 10^{-4}$ *M* (14), $1.5 \cdot 10^{-4}$ *M* (15), and $5.0 \cdot 10^{-4}$ *M* (16). (c) Absorption spectra of acidified solutions of DMA-DPPQ ($c = 5 \cdot 10^{-5}$ *M*) in ethanol. $HClO_4$ concentrations: 0 *M* (1), $2.5 \cdot 10^{-3}$ *M* (2), $5.0 \cdot 10^{-3}$ *M* (3), $1.0 \cdot 10^{-2}$ *M* (4), $2.0 \cdot 10^{-2}$ *M* (5), and $9.0 \cdot 10^{-2}$ *M* (6).

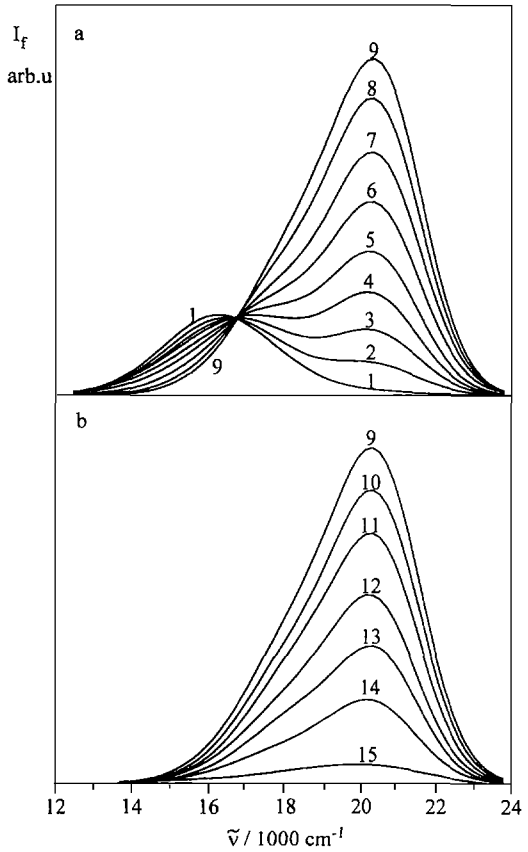

Fig. 9. Corrected fluorescence spectra of DMA-DPPQ ($c = 5 \cdot 10^{-5}$ *M*) in acidified acetonitrile solutions: (a) $HClO_4$ concentrations from 0 *M* (1) to $4 \cdot 10^{-5}$ *M* (9). The increment of the acid concentration is $0.5 \cdot 10^{-5}$ *M*. (b) $HClO_4$ concentrations: $5.0 \cdot 10^{-5}$ *M* (10), $6.0 \cdot 10^{-5}$ *M* (11), $8.0 \cdot 10^{-5}$ *M* (12), $1.0 \cdot 10^{-4}$ *M* (13), $1.5 \cdot 10^{-4}$ *M* (14), and $5.0 \cdot 10^{-4}$ *M* (15).

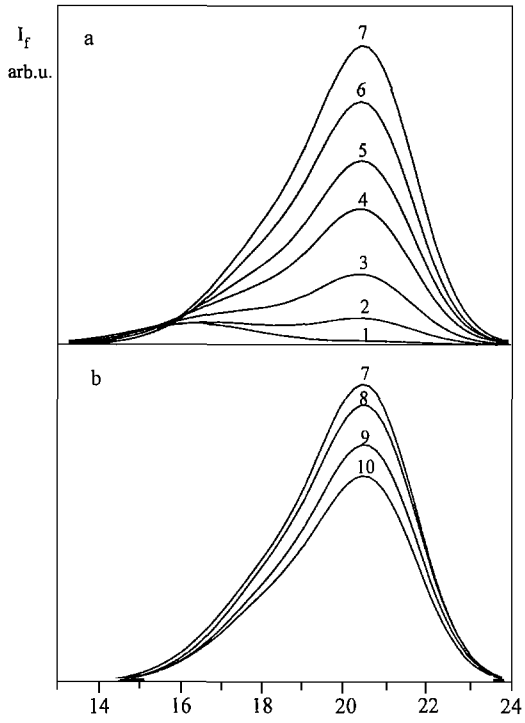

Fig. 10. Corrected fluorescence spectra of DMA-DPPQ ($c = 5 \cdot 10^{-5}$ *M*) in ethanol solutions. $HClO_4$ concentrations: (a) 0 *M* (1), $1.0 \cdot 10^{-3}$ *M* (2), $2.5 \cdot 10^{-3}$ *M* (3), $5.0 \cdot 10^{-3}$ *M* (4), $7.5 \cdot 10^{-3}$ *M* (5), $1.2 \cdot 10^{-2}$ *M* (6), and $2.0 \cdot 10^{-2}$ *M* (7); (b) $2.0 \cdot 10^{-2}$ *M* (7), $5.0 \cdot 10^{-2}$ *M* (8), $7.0 \cdot 10^{-2}$ *M* (9), and $9.0 \cdot 10^{-2}$ *M* (10).

mol^{-1} higher in energy than the vertically excited S_1 state. The eighth excited state for the conformation with a twisted dimethylamino group is of even larger charge transfer character ($\mu = 110 \cdot 10^{-30}$ Cm), which is best described by an electron transfer from the free electron pair located on the amino nitrogen to the π^* orbitals of the heteroaromatic unit and large contributions arising from the distant γ phenyl groups.

The orientation of the transition dipole moment for the first, second, and third excited states are calculated using the pairwise excited configuration interaction (PECI) [20] method and the results are summarized in Table II. The S_2 dipole moment is oriented along the *x* axis and inclined by an angle of approximately 60° to that of S_1, and by 80° to that of the S_3 state, and the S_4 dipole moment coincides with the *y* axis (for assignment of the molecular axes see also Scheme II).

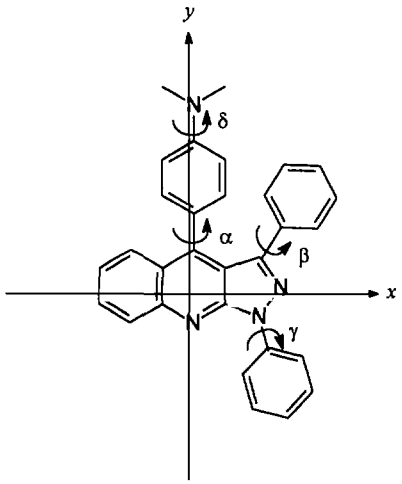

Scheme II

Self-consistent reaction field (SCRF) calculations in the polar but aprotic solvent acetonitrile and in apolar hexane are carried out in order to investigate the state energies and the dipole moments in a solvated medium.

Table I. Total Energies (kJ mol^{-1}) and Dipole Moments (10^{-30} Cm) of the Ground and First DMA-DPPQ Excited States from Different Reference Geometries[a]

	Optimized (α = 74°)		Unwagged (ω = 0°)		Twisted (δ = 90°)	
	ΔH_f	μ	ΔH_f	μ	ΔH_f	μ
S_0	932.8	15.0	934.5	16.0	959.3	9.7
S_1	1254.4	13.7	1253.2	41.0	1271.2	6.3
S_3	1329.8	37.0	1321.8	37.0	1306.8	60.4

[a] The ground-state energies are computed without electron correlation effects.

Table II. Transition Dipole Moment for the Six Lowest Excited States of DMA-DPPQ

	x	*y*
S_1	0.55	0.94
S_2	0.29	0.01
S_3	0.27	1.18
S_4	−0.01	−1.38
S_5	1.46	−0.11
S_6	−0.83	0.40

Table III. Calculated Total Energies (kJ mol^{-1}) and Dipole Moments (10^{-30} Cm) of the First DMA-DPPQ Excited Sates (α = 90°) in Gas Phase, in Hexane, and in Acetonitrile

	Gas phase		Hexane		Acetonitrile	
	ΔH_f	μ	ΔH_f	μ	ΔH_f	μ
S_0	887.2	16.0	875.0	18.7	871.3	21.0
S_{LE}	1256.5	11.3	1241.8	8.7	1237.6	12.7
S_{CT}	1529.0	81.7	1242.6	99.1	1157.7	99.1

The results are summarized in Table III. The partial charge transfer character for the third excited state yields its maximum dipole moment of 82 · 10^{-30} Cm for completely decoupled donor acceptor subunits (α = 90°). This state is destabilized in total energy relatively to the ground-state energy by ΔH_f = 1529.0 kJ mol^{-1}, in contrast to 1330 kJ mol^{-1} for α = 74°. The high polarizability of this state increases its dipole moment from 81.7 · 10^{-30} to 99.1 · 10^{-30} Cm in solution. The charge transfer state is significantly stabilized in energy by solute–solvent interactions of this highly polar excited state. The S_{CT} is lowered to the energy of the first excited state [ΔH_f (S_{LE}) = 1241.8 kJ mol^{-1} and ΔH_f(S_{CT}) = 1242.6 kJ mol^{-1}] and below the S_{LE} energy in solvents of higher polarity, e.g., in acetonitrile where the polar state is 80 kJ mol^{-1} lower in energy than the locally excited state. This stabilisation results in a change of the emitting state for different environment. The LE state is the lowest excited state in apolar solvents, whereas the CT state becomes more feasible in energy in solvents of higher polarity. The increasing stabilization corresponds to a red-shift computed for polar solvents. The short wavelength emission calculated at 30,600 cm^{-1} (327 nm) undergoes a significant red shift. In acetonitrile, for example, for a polar solvent the computed emission energy is found at 20,060 cm^{-1} (499 nm).

Decoupling of donor and acceptor subunits by twisting of the dimethylamino group (δ) by 90° increases the dipole moment, which increases significantly in a polar environment. The total energy of this so-called TICT state is thereby lowered to an energy near to that of the first excited state due to electrostatic interactions of the solvent (μ = 108 · 10^{-30} Cm).

Calculations of the net atomic charges yield a maximal electron density at the amino group, decreasing to half a net charge at the pyridine nitrogen and almost no negative charge located on the aza nitrogen atoms. Calculation of ground and excited state energies of the protonated forms shows the pyridine ring as the preferential site for protonation. This species is lower in total energy compared to the aza protonated form by approximately 63 kJ mol^{-1} in both the ground and the first excited state. Amino nitrogen protonation is also disfavored in the ground as well as in the excited state.

For the other three compounds the ground-state dipole moments are pointing in the same direction as for DMA-DPPQ but have smaller values, i.e., 15 · 10^{-30} Cm for DMA-BIPPQ and DMA-2NAPPQ and 6.7 · 10^{-30} Cm in the case of H-DPPQ. The S_1 dipole moment for two other donor-substituted compounds rotate in comparison to DMA-DPPQ and the component along the *x* axes vanishes for DMA-BIPPQ [$\mu(S_1)$ = 10 · 10^{-30} Cm] and becomes negative for DMA-2NAPPQ [$\mu(S_1)$ = 16 · 10^{-30} Cm]. The dipole moment of H-DPPQ changes only its direction upon excitation: the vector has positive *xz* direction in the ground state but negative ones in the excited state. Its value remains, however, unchanged, equal to 6.3 · 10^{-30} Cm.

DISCUSSION

Effects of solvent polarity on absorption and fluorescence properties are studied for various donor-substituted phenylpyrazoloquinolines and for the parent

compound. The first absorption band shows generally different negative solvatochromism, i.e., a blue-shift with increasing solvent polarity. On the contrary, fluorescence shows positive solvatochromism. A blue-shift of the spectrum with increasing polarity might be caused either (i) by a substantial change in the direction of the dipole moment upon excitation (or ii) deviations of the interactions between the dipole moment in the ground and/or excited state and the reaction field generated by the environment from Onsager's model [7]. The first case is easy to explain according to Eqs. (1) and (2):

$$\tilde{\nu}_{abs} = \tilde{\nu}^0_{abs} - \frac{\vec{\mu}_n\,(\vec{\mu}_m - \vec{\mu}_n)}{4\pi\varepsilon_0 hc\chi a^3} * \Delta f \qquad (2)$$

Equation (2) is obtained analogously to Eq. (1). The experimentally observed blue-shift of the absorption spectrum, which is maximal for H-DPPQ but decreases for DMA-BIPPQ and DMA-2NAPPQ and even more for DMA-DPPQ, i.e., with decreasing size of the aromatic substituent, might be attributed to reorientation of the dipole moments in the first excited state, according to Eq. (2). Semiempirical calculations yield an inversion of the direction of the dipole moment upon excitation for the parent compound H-DPPQ: the angle between the dipole moment in the S_0 ground state and the S_1 excited state is near 180°. For the donor-substituted compounds this angle between two vectors becomes smaller and decreases in the respective order of the experimental blue-shift: it is significantly smaller than 180° for DMA-2NAPPQ but larger than for DMA-BIPPQ and DMA-DPPQ. Substantial reorientation of the dipole moments upon excitation, suggested by the spectral shifts, is thus reproduced by the semiempirical calculations.

The characteristics of the fluorescent state of the donor-substituted compounds change significantly with increasing solvent polarity. In solvents less polar than 1-chlorobutane, i.e., for a polarity function $\Delta f < 0.2$, the observed solvent shift is much smaller than at higher polarities, and this can be interpreted as that fluorescence occurs from a considerably less polar state in low polar solvents. Also, other photophysical parameters like Q_F decrease significantly in the same polarity range (see Fig. 6), and this corroborates this change in the emissive state. This effect is, however, not observed for the parent compound H-DPPQ: The fluorescence shift changes linearly with Δf, and Q_F remains large.

The state emissive in the low-polarity regime is identical to the vertically excited S_1 state which arises from an excitation located mainly on the H-DPPQ moiety, and this is also in good agreement with theoretical considerations. The transition dipole is oriented along the long axis of this subunit and does not change upon excitation. This is clearly demonstrated by the fluorescence anisotropy, which is near the theoretical limit of 0.4 for the lowest excitation. The transition dipole of the next higher excited state changes its orientations significantly, as it is nearly orthogonal to that of the S_1 state and also considerably smaller in length. This is also in good agreement with the experimental results.

Vertical excitation significantly changes the orientation of the molecular dipole moment. This was discussed above in relation to the observed spectral shifts. A change in the dipole moments of $\Delta\mu_{mn} = 34 \cdot 10^{-30}$ Cm results from the shift of the fluorescence spectra assuming that the ground and excited states are oriented parallel or antiparallel, nearly identical for all compounds at low solvent polarities. This value is near the sum of the ground- and excited-state dipole moments, which are obtained from semiempirical calculation, and this corroborates the result that in the ground and excited state dipole moments are oriented nearly antiparallel, at least for the parent compound. The length of the dipole moment does not change significantly upon excitation.

An excited state with a much larger dipole moment is, however, emissive in the high-polarity regime. The spectral shift increases significantly and the photophysical parameters changes dramatically [12]. The large dipole moment, which reaches nearly $90 \cdot 10^{-30}$ Cm, and the strong decrease in the fluorescence yield indicate an intramolecular change transfer state to be the emissive species in the donor-substituted compounds at high solvent polarities. A respective state characterized by the transfer of an electron from the dimethylamino donor group to the DPPQ acceptor moiety is found as S_3 in the semiempirical calculations. It is most likely that this state becomes the lowest excited state as the solvent polarity increases. The excited-state dipole moment is already large for the optimum ground-state geometry, in which the angle between donor and acceptor moieties is larger than 70° and increases slightly in the orthogonal arrangement. Excited-state relaxation along the α coordinate might thus occur in a polar solvent but is not essential to obtain intramolecular change separation. Most important, however, is reorientation of the solvent dipoles, as the molecular dipole moments in ground and vertically and relaxed excited states are oriented in different directions.

Excited-state solvent reorientation might explain the observation of dual fluorescence in hydroxylic solvents. Solvent relaxation is relatively slow in alcohols and fluorescence from the nonrelaxed highly fluorescent state might effectively compete with relaxation. As the yield of the fluorescence originating from the relaxed

state is low, dual fluorescence becomes observable in alcohols.

The importance of solvent reorientation in the emissive state is also clearly indicated by the results from low-temperature fluorescence measurements. In butyronitrile solution relaxation to the charge-separated state is efficient at all temperatures, and only in glassy solutions at 146 K are some indications for dual fluorescence found (see Fig. 7). The fluorescence quantum yield is low and remains nearly constant over the whole temperature range. The spectrum shifts concomitantly with increasing solvent polarity and decreasing temperature, as long as the solution does not form a glass. The picture is completely reverse for solutions in propanol-1, a solvent with a much higher viscosity, which additionally increases considerably at low temperatures [21]. Solvent reorientation is thus much slower in this environment and becomes inefficient at 132 K. At this temperature only high-energy emission originating from the primary excited state is observed with high fluorescence yield. As the temperature increases, relaxation to the charge-separated state competes with fluorescence from the nonrelaxed state, and two strongly overlapping bands are observed. The fluorescence yield decreases accordingly and dual fluorescence becomes observable when the temperature is sufficiently high to allow fast solvent relaxation.

Additional information on the nature of the emissive state and on the solvent relaxation processes operative in different media stems from the investigation of the protonation effects on the fluorescence properties in a nonaqueous environment. Well-defined isosbestic points are found in the absorption spectra and they suggest that equilibrium between protonated and nonprotonated forms is established in the ground state (see Fig. 8). The appearance of a new long-wavelength band could be interpreted as a protonation of the quinoline nitrogen. The pyridinium and the quinolinium cations absorb at longer wavelengths than the corresponding nonprotonated compounds [22]. No fluorescence is observed upon excitation of this band. The spectrum is thus a composite of several protonated forms and protonation of the pyridinium nitrogen yields a nonfluorescent product.

An increase in acid concentration (see Fig. 8a) causes an increase in a short-wavelength fluorescence band similar to that of the parent compound H-DPPQ. The dominating processes protonation is thus most likely protonation of the amino nitrogen of the dimethylanilino group. This reduces effectively the possibility of intramolecular charge transfer, and only the high-energy band is thus observed in the fluorescence. This view is corroborated by semiempirical calculations showing that the electronic aspects definitely favor the formation of the dimethylamino protonated species and of the pyridine nitrogen, to a lesser extent, in agreement with experiment.

The molecule protonated on the amino nitrogen emits at shorter wavelengths than the unprotonated species, as no charge-transfer state can be formed and at a molar concentration ratio of DMA-DPPQ/$HClO_4$ 1:1 an intensive fluorescence band ($Q_F > 0.7$) with a maximum at 20,300 cm^{-1} is observed. H-TPPQ (1,3,4-triphenylpyrazolo[3,4-*b*]quinoline) fluoresces at a similar wavelength, i.e., at 21,600 cm^{-1} in isooctane and at 21,200 cm^{-1} in ethanol [8]. The large quantum yields of the 20,300 cm^{-1} fluorescence indicates that almost all DMA-DPPQ molecules are protonated in the ground state and emit without dissociation of the proton in the excited state. This was just not expected because of the well-known eminent increase in acidity of aromatic amines in their first excited singlet state.

This behavior can be explained as the result of the inability of acetonitrile to act as a proton acceptor. Thus no equilibrium is established in the excited state. The dual fluorescence in acidified solutions reflects the ground-state equilibrium. In the second step of protonation the other set of isosbestic points is observed (Fig. 8b), most probably corresponding to the equilibrium monocation (protonated at amino nitrogen) $\leftrightarrows$ bication (additionally protonated at one aza nitrogen). At this step only the quenching of the 20,300 cm^{-1} fluorescence is observed; lack of emission ability of bication therefore has to be concluded.

In ethanol as solvent the protonation is similar to that in acetonitrilic solutions, but the same spectral changes are obtained at higher $HClO_4$ concentrations than in the latter case (Fig. 8c). The isoemissive points are observed in the first step of protonation (see Figs. 9a and 10a), although the solutions were excited at the maximum absorption band at 24,000 cm^{-1}. The absorbance of this energy decreases strongly (see Figs. 8a and 8c) upon the addition of acid. The decrease in the amount of absorbed photons has to be compensated, however, by a concomitant increase in quantum yields of the protonated form with increasing acid concentration. Indeed, the fluorescence lifetime increases with increasing $HClO_4$ concentration. It equals 10.4 ns for the nonprotonated DMA-DPPQ molecule in acetonitrile, whereas in acidified solution (ratio of acid/solute, 0.8) it is 30.0 ns.

The red-shift of the fluorescence band in cooled butyronitrilic solutions and the blue-shift of the long-wavelength band in propanolic solutions can be rationalized by the larger relaxation time of propanol-1 than that of butyronitrile at temperatures below 272 K. Unexpect-

edly, the fluorescence in glassy butyronitrile occurs at an energy only negligibly lower than that at room temperature. It suggests that factors other than polarity of the environment have to control the large Stokes shift of the fluorescence in this case. In solidified propanol solution the short-wavelength band is observed exclusively at the energy corresponding to that of fluorescence in nonpolar solvents. The different excitation spectra of both fluorescence bands in alcohols suggest the existence of two species. Most probably one of them is hydrogen bonded and unable to relax to the CT state. The second species can be solvated in a favorable way for the relaxation. However, the decrease in polarity of propanol-1 at low temperatures retards the relaxation; therefore, the short-wavelength fluorescence increases. At the present stage we cannot define its nature and ascribe it to hydrogen-bonded and nonbonded species and/or nonrelaxed primary excited state, interacting nonspecifically with solvent. It is noteworthy that in mixed binary aprotic solvents (e.g., toluene/acetonitrile), a single fluorescence is observed [12]. The spectrum shifts to red with increasing acetonitrile concentration. In the mixture of heptane/butanol-1 dual fluorescence occurs. The short-wavelength band decreases with increasing concentration of butanol-1. This fact corroborates the interpretation of the appearance of the short-wavelength band as a result of hydrogen complexation of the DMA-DPPQ molecule in the ground state.

CONCLUSIONS

The experimentally observed blue-shift of the absorption spectra can be explained by a significant change of the orientation of the dipole moment upon excitation and this is also found by theoretical calculations. Donor-substituted derivatives of pyrazoloquinoline (DMA-DPPQ, DMA-BIPPQ, and DMA-2NAPPQ) show intensive fluorescence in low-polar and medium-polar solvents, which is emitted from the primary excited state, a relatively polar state located on the DPPQ acceptor moiety. The fluorescence quantum yield decreases with increasing solvent polarity and the dipole moment of the emitting state increases dramatically. This corresponds to an inversion of states and the third excited state with intramolecular charge transfer character becomes the fluorescing state. This is in good agreement with quantum chemical calculations. Dual fluorescence originating from these two states is observed in polar protic solvents and can be related to slow solvent reorientation in alcohols. The identification of two emissive states of different charge-transfer character is further corroborated by the study of protonation effects in nonaqueous solvents. First, the amino group nitrogen atom is preferentially protonated and this prevents intramolecular charge transfer. A second step of protonation, most likely on the azanitrogens, is also observed, connected with efficient fluorescence quenching. No dissociation of the protonated species upon excitation is found in the nonaqueous solvents.

ACKNOWLEDGMENTS

K. Rechthaler, A. Parusel, and G. Köhler thank the Fond zur Förderung der wissenschaftlichen Forschung in Österreich (Project Nr. P11880-CHE) for financial support. The work was partially supported by Austrian–Polish Project 01-003 and Grant 8T11b00510 from the Committee for Scientific Research (Poland).

REFERENCES

1. W. Rettig (1986) *Angew. Chem. Int. Ed. Engl.* **25**, 971.
2. W. Rettig (1994) in J. Mattay (Ed.), *Topics in Current Chemistry*, Springer, Berlin, p. 253.
3. Z. R. Grabowski, K. Rotkiewicz, A. Siemiarczuk, D. J. Cowley, and W. Baumann (1979) *Nouv. J. Chim.* **3**, 443.
4. S. R. Marder, B. Kippelen, A. K-Y. Jen, and N. Peyghambarian (1997) *Nature* **388**, 845.
5. J. Herbich and A. Kapturkiewicz (1991) *Chem. Phys.* **158**, 143.
6. J. Herbich and A. Kapturkiewicz (1993) *Chem. Phys.* **170**, 221.
7. A. Kapturkiewicz, J. Herbich, J. Karpiuk, and J. Nowacki (1997) *J. Phys. Chem. A* **101**, 2332.
8. G. Grabner, K. Rechthaler, and G. Köhler (1998) *J. Phys. Chem. A* **102**, 689.
9. K. Rotkiewicz, K. Rechthaler, A. Puchała, D. Rasała, S. Styrcz, and G. Köhler (1996) *J. Photochem. Photobiol. A Chem.* **98**, 15.
10. A. B. J. Parusel, R. Schamschule, D. Piorun, K. Rechthaler, A. Puchała, D. Rasała, K. Rotkiewicz, and G. Köhler (1997) *J. Mol. Struct. (THEOCHEM)* **419**, 63.
11. A. B. J. Parusel, R. Schamschule, and G. Köhler (1997) *Ber. Bunsenges. Phys. Chem.* **101**, 1836.
12. K. Rechthaler, K. Rotkiewicz, A. Danel, P. Tomasik, and K. Khatchatryan (1997) *J. Fluoresc.* **7**, 301.
13. D. Tomasik, P. Tomasik, and R. A. Abramovitch (1983) *J. Heterocycl. Chem.* **20**, 1539.
14. A. Danel, K. Khatchatryan, and P. Tomasik (unpublished).
15. J. Jasny (1978) *J. Luminescence* **17**, 149.
16. M. J. S. Dewar, E. G. Zoebisch, E. F. Healy, and J. J. P. Stewart (1985) *J. Am. Chem. Soc.* **107**, 3902.
17. G. Rauhut, A. Alex, J. Chandrasekhar, T. Steinke, W. Sauer, B. Beck, M. Hutter, P. Gedeck, and T. Clark (1997) *VAMP6.1*, Oxford Molecular, Oxford.
18. G. Rauhut, T. Clark, and T. Steinke (1993) *J. Am. Chem. Soc.* **115**, 9174.
19. G. Köhler, P. Wolschann, and K. Rotkiewicz (1992) *Proc. Indian Acad. Sci. (Chem. Sci.)* **104**, 197.
20. T. Clark and J. Chandrasekhar (1993) *Israel J. Chem.* **33**, 435.
21. D. R. Lide (ed.), *CRC Handbook of Chemistry and Physics (1992/93)*, 73rd ed., CRC Press, Boca Raton, FL, pp. 6–167; M. Maroncelli (1993) *J. Mol. Liq.* **57**, 1.
22. W. W. Simons (Ed.) (1979) *The Sadtler Handbook of Ultraviolet Spectra*, Sadtler Research Laboratories, Philadelphia, p. 154.